International Electronic Journal of Pure and Applied Mathematics

Volume 5 No. 4 2012, 157-172

STABILITY DOMAINS FOR STATIC SOLUTIONS IN SYMMETRIC 0-π JOSEPHSON JUNCTION

J.A. Angelova[1] §, T.L. Boyadjiev[2]

[1]Department of Mathematics
University of Chemical Technology and Metallurgy
8, Kl. Ohridski, Blvd, Sofia, 1756, BULGARIA

[2]Joint Institute for Nuclear Research
Dubna, 141980, RUSSIAN FEDERATION

Abstract: We calculate numerically the stability boundaries of various types of static solutions for symmetric 0-π long Josephson junction. Then the dependence of the critical current γ_c versus applied magnetic field h_e can be reconstructed. We investigate the $\gamma_c(h_e)$ as a function of the junction length and find some new features related to the asymmetric solutions. Our results allow to associate different branches on experimentally measured $\gamma_c(h_e)$ with a particular type of solution. The dependence of the critical current γ_{c0} at $h_e = 0$ as a function of the Josephson junction's length is numerically obtained. The numerical results agree with known experimental data.

AMS Subject Classification: 81T80, 82D55, 82D40, 74F15, 70K50, 34K10
Key Words: Josephson junction, sine-Gordon equation, numerical modeling, vortex, semifluxon, 0-pi junction stability, bifurcation

Introduction

The possibility of having π phase shift in the ground state of the Josephson junction (JJ) was predicted long ago [1]. Nowadays, physicists are able to fabricate and study several types of π JJs based on different physical principles [4, 2, 3].

An interesting system can be created by combining conventional (0) and π JJs in one device — the so-called 0-π JJs [5]. Not only 0 and π parts compete with each other resulting in new type of the ground states, but also long 0-π JJs can have vortices carrying only half of the magnetic flux quantum Φ_0. A significant number of

Received: November 28, 2012

§Correspondence author

International Electronic Journal of Pure and Applied Mathematics – IEJPAM, Volume 5, No. 4 (2012)

theoretical and experimental works studying 0-π JJs were published during the last decade, see [6] – [9], [13] – [18] and references therein. In particular, experimentally measured dependence of the critical current versus externally applied magnetic field for 0-π JJs were modeled numerically [19, 13].

In general, the transitions from static to dynamic state upon changing the external current γ are mathematically interpreted as a bifurcation of one of the possible static solutions $\varphi(x)$ existing in the junction at given external magnetic field h_e (from now on all the variables are dimensionless).

In this paper we numerically investigate the stability boundaries of various types of static solutions for symmetric 0-π long JJ (LJJ) on the plane "critical current – applied magnetic" field. The critical curve of the contact is obtained as an envelope of the bifurcation curves corresponding to different static solutions.

The paper is organized as follows. In Section 1 we introduce a mathematical model, state the problem and describe the technique used to obtain the solutions. The main numerical results for static vortex solutions and their bifurcations are presented in Section 2. The final Section 3 concludes the work.

1. Statement of the Problem

1.1. Model

Consider a 0-π Josephson junction of length $2l$ ($l < \infty$), disposed along x axis, such that the 0-JJ is situated at $x < 0$ and π-JJ is situated at $x > 0$. Distribution of the Josephson phase $\varphi(x)$ along JJ is governed by the sine-Gordon equation supplemented by the boundary conditions. In the case of overlap geometry this non-linear boundary value problem (BVP) for static distributions of the phase $\varphi(x)$ can be written as

$$-\varphi_{xx} + j_C(x)\sin\varphi - \gamma = 0, \quad x \in (-l, l) \setminus \{0\}, \tag{1.1a}$$

$$\varphi(-0) = \varphi(+0), \tag{1.1b}$$

$$\varphi_x(\zeta - 0) = \varphi_x(\zeta + 0), \tag{1.1c}$$

$$\varphi_x(\pm l) = h_e\,, \tag{1.1d}$$

where $j_C(x)$ is the critical current density

$$j_C(x) = \begin{cases} 1, & x \in [-l, 0]; \\ -1, & x \in (0, l]\,. \end{cases}$$

The sine-Gordon equation (1.1a) is the Euler-Lagrange equation of the field with Lagrangian density

$$\mathcal{L}(\varphi) = \frac{1}{2}\varphi_x^2 + j_C(x)\,(1 - \cos\varphi) - \gamma\varphi \tag{1.2}$$

International Electronic Journal of Pure and Applied Mathematics – IEJPAM, Volume 5, No. 4 (2012)

at corresponding subintervals.

The possible solutions φ of (1.1) are twice continuously differentiable functions except at $x = 0$, $\varphi \in C^2\{[-l, l] \setminus \{0\}\}$. Physically this means that the magnetic field inside the junction is continuous only, and at the sewing point $x = 0$ continuity conditions (1.1b) and (1.1c) are fulfilled [8]–[15].

One can check that for $\gamma = 0$ the common solution of equations (1.1a) in the corresponding intervals is expressed by the elliptic functions, see [**?**]. Under the given model's parameters $p = \{l, h_e, \gamma\}$ the integration constants can be obtained by means of two boundary conditions (1.1d) and two continuity conditions (1.1b) and (1.1c) [21].

For small magnitudes of the current $|\gamma| \ll 1$ the solution of the BVP (1.1) can be derived applying perturbation theory methods. In more general cases the solutions of arising non-linear systems for integration constants can be obtained only numerically, as in the present paper.

1.2. Stability of Static Solutions

From now on we suppose continuous dependence of solutions $\varphi = \varphi(x, p)$ of (1.1) on parameters. So, we will say that the solutions $\varphi_1(x, p_1)$ and $\varphi_2(x, p_2)$ belong to the same type if $\varphi_1(x, p_1)$ smoothly transforms into $\varphi_2(x, p_2)$ upon continuous change of p from p_1 to p_2. The dependence of the solutions $\varphi(x, p)$ on p we will write explicitly only if it is necessary.

The non-linear BVP (1.1) for $\varphi(x)$ and (1.2) can be considered as system of equations, which represent the necessary conditions for extrema of the total energy functional $F[\varphi]$ of the junction

$$F[\varphi] = \int_{-l}^{l} \mathcal{L}(\varphi)\, dx - h_e \Delta\varphi\,, \tag{1.3}$$

where functions φ are of class $C^2\{[-l, l] \setminus \{0\}\}$ and the total dimensionless magnetic flux $\Delta\varphi$ through the junction is defined as

$$\Delta\varphi = \int_{-l}^{l} \varphi_x\, dx = \varphi(l) - \varphi(-l)\,. \tag{1.4}$$

The Weierstrass-Erdmann conditions yield (1.1d), (1.1b), and (1.1c), see [**?**].

A regular Sturm-Liouville problem (SLP) associated with our BVP is set as

$$-\psi_{xx} + q(x)\psi = \lambda\psi, \quad x \in (-l, l) \setminus \{0\}, \tag{1.5a}$$

$$\psi(-0) = \psi(+0), \tag{1.5b}$$

$$\psi_x(-0) = \psi_x(+0), \tag{1.5c}$$

International Electronic Journal of Pure and Applied Mathematics – IEJPAM, Volume 5, No. 4 (2012)

$$\psi_x(\pm l) = 0\,, \tag{1.5d}$$

$$\int_{-l}^{l} \psi^2(x)\,dx = 1\,, \tag{1.5e}$$

where $q(x) = j_C(x)\cos\varphi(x)$ is a potential and (1.5e) is a normalizing condition for the uniqueness of eigenfunctions $\psi(x)$. The SLP (1.5) determines the stability of static solutions $\varphi(x)$ (we assume that the time-dependent solution $\varphi(x,t)$ deviates a little from the static solution) and is related to the sufficient conditions for extrema of $F[\varphi]$. If, for some solution $\varphi(x)$ of BVP, the minimum eigenvalue $\lambda_0 > 0$ of SLP, then the second variation of $F[\varphi]$ around this solution is positive and F has a minimum at $\varphi(x)$. Therefore, the solution $\varphi(x)$ is linearly stable [32]. Such approach for "one-dimensional" LJJs was proposed in [20, 21] and discussed in many works, see for example [22] – [30]. A similar method in case of 0-π JJ was used in [6], [23].

For SLP (1.5), there exists a non-degenerate discrete spectrum of possible λ values bounded from below, i.e.,

$$-1 \le \lambda_0 < \lambda_1 < \cdots < \lambda_n < \ldots\,, \tag{1.6}$$

because $|q(x)| \le 1$ for $x \in [-l, l]$, see [31]. Since $\varphi(x,p)$ depends on p, then λ_n and ψ_n also depend on p, and if $\lambda_n(\varphi(x,p)) > 0$ (or $\lambda_n(\varphi(x,p)) < 0$) then the corresponding solution $\varphi(x,p)$ is stable (or unstable). Obviously, if at least one of λ_n for fixed static $\varphi(x,p)$ is negative, then the whole solution $\varphi(x,p)$ is unstable. Since λ_n are arranged according to (1.6), the stability/instability boundary (bifurcation point) is defined as

$$\lambda_0(\varphi(x,p)) = 0\,. \tag{1.7}$$

It is convenient to interpret the last equation geometrically as a surface in the parameters space. Each point on this surface is a bifurcation (critical) point for the solution $\varphi(x,p)$. In this paper we consider $\lambda_0(\varphi(x,h_e,\gamma))$ so that (1.7) gives explicit dependence of $\gamma_c(h_e)$ for each type of the static solution. We note, that similar study for 0-JJs [28], [29] and for 0-π JJs [11] was already undertaken.

1.3. Algorithm and Computing

In this article we apply algorithms proposed in [35, 36] to derive numerically the relation (1.7) (see also review [27]). The BVP (1.1) and nonlinear SLP (1.5) include parameter h_e and λ, respectively, on right hand side of equations and can rewrite as one vector functional equation

$$\overrightarrow{f}(\varphi, \psi, h_e) = \overrightarrow{0}\,. \tag{1.8}$$

International Electronic Journal of Pure and Applied Mathematics – IEJPAM, Volume 5, No. 4 (2012)

To find eigenvalues and eigenfunctions $(\varphi(x), \psi(x))$ we use the method based on continuous analogue to Newton method (CANM) [37], which yield equations:

$$\begin{aligned} \overrightarrow{f}'_{\varphi}\Phi + \overrightarrow{f}'_{\psi}\Psi + \overrightarrow{f}'_{h_e}H + \overrightarrow{f}(\varphi,\psi,h_e) &= \overrightarrow{0}, \\ \Phi &= \dot{\varphi}, \\ \Psi &= \dot{\psi}, \\ H &= \dot{h_e}, \end{aligned} \tag{1.9}$$

where $\overrightarrow{f}'_{\varphi}$, $\overrightarrow{f}'_{\psi}$, $\overrightarrow{f}'_{h_e}$ are Fréchet derivatives. In case under consideration they coincide with corresponding partial derivatives. By type of (1.8) it follows that solutions of (1.9) can search as

$$\begin{aligned} \Phi =& \xi + H\eta, \\ \Psi =& \varsigma + H\chi, \end{aligned} \tag{1.10}$$

where ξ, η, ς, χ are new variables. Substituting (1.10) in (1.9) the above equations are reduced, see e.g. [33], to four eigenvalues problems:

$$\begin{aligned} \xi_x(-l) &= h - \varphi_x(-l), \\ -\xi_{xx} + \cos\varphi\,\xi &= \varphi_{xx} - \sin\varphi + \gamma, \\ \xi\,(+0) - \xi(-0) &= \varphi(-0) - \varphi(+0), \\ \xi_x\,(+0) - \xi_x\,(-0) &= \varphi_x\,(-0) - \varphi_x\,(+0)\,, \\ -\xi_{xx} - \cos\varphi\,\xi &= \varphi_{xx} + \sin\varphi + \gamma, \\ \xi_x\,(l) &= h - \varphi_x(l); \end{aligned} \tag{1.11}$$

$$\begin{aligned} \eta_x(-l) &= 1, \\ -\eta_{xx} + \cos\varphi\,\eta &= 0, \\ \eta\,(+0) - \eta\,(-0) &= 0, \\ \eta_x\,(+0) - \eta_x\,(-0) &= 0, \\ \eta_{xx} + \cos\varphi\,\eta &= 0, \\ \eta_x\,(l) &= 1; \end{aligned} \tag{1.12}$$

$$\begin{aligned} \zeta_x(-l) &= 0, \\ -\zeta_{xx} + (\cos\varphi - \lambda)\,\zeta &= \psi_{xx} + (\lambda - \cos\varphi) + \sin\varphi\,\psi\,\xi, \\ \zeta\,(+0) - \zeta\,(-0) &= 0, \\ \zeta_x\,(+0) - \zeta_x\,(-0) &= 0, \\ \zeta_{xx} + (\cos\varphi - \lambda)\,\zeta &= -\psi_{xx} + (\lambda - \cos\varphi) + \sin\varphi\,\psi\,\xi, \\ \zeta_x\,(l) &= 0; \end{aligned} \tag{1.13}$$

International Electronic Journal of Pure and Applied Mathematics – IEJPAM, Volume 5, No. 4 (2012)

$$\begin{aligned} \chi_x(-l) &= 0, \\ -\chi_{xx} + (\cos\varphi - \lambda)\ \chi &= \sin\varphi\,\psi\,\eta, \\ \chi\,(+0) - \chi\,(-0) &= 0, \\ \chi_x\,(+0) - \chi_x\,(-0) &= 0, \\ \chi_{xx} + (\cos\varphi - \lambda)\ \chi &= \sin\varphi\,\psi\,\eta, \\ \chi_x\,(l) &= 0; \end{aligned} \tag{1.14}$$

and a norm condition implication

$$H = \left(2 \int_{-l}^{l} \psi(x)\chi(x)\,dx \right)^{-1} \left\{ 1 - \int_{-l}^{l} \left[\psi^2(x) + 2\psi(x)\zeta(x) \right]\,dx \right\}. \tag{1.15}$$

The discretization of corresponding linearized eigenvalues BVPs (1.11) – (1.14) is performed by means of spline-collocation method, see e.g. [34]. Such approach leads to difference scheme with block three-diagonal matrix. The scheme's accuracy is $O(h^4)$ determined by Runge's method on the sequence of uniform meshes with steps h, $h/2$ and $h/4$.

2. Results

2.1. Static Vortex Solutions

First let's consider some solutions of (1.1) (far enough from the bifurcation point) and behavior of their main physical characteristics when parameters tend to the critical values.

Figures 1 and 2 show stable semifluxon-like solutions $\varphi_0(x)$ in 0-π JJ at two values of l. For convenience, we shall use the notation $\Phi^{\pm 1/2}$ to denote this type of solutions. $\Phi^{+1/2}$ is a semifluxon-like solution (full semifluxon is obtained at $l \to \infty$), while $\Phi^{-1/2}$ is antisemifluxon-like solutions. If p changes, but does not pass the bifurcation point, the $\varphi_0(x,p)$ changes too, but the solution type remains the same. Therefore, we will often write, e.g., $\Phi^{\pm 1/2}(x)$ if we want to refer to all solutions $\varphi_0(x)$ of this type. As predicted earlier, see [5], these states have: (a) finite total magnetic flux ($\Delta\varphi \approx \pm 0.147$ at $2l = 2$, $\Delta\varphi \approx \pm 0.468$ at $2l = 7$, respectively); (b) finite energy ($F[\Phi^{\pm 1/2}] \approx -0.04$ at $2l = 2$, $F[\Phi^{\pm 1/2}] \approx -0.583$ at $2l = 7$) and (c) average phase $N[\Phi^{\pm 1/2}] = \pm 1/2$ see (2.1). The functional $N[\varphi]$ is introduced in [38] as

$$N[\varphi] = \frac{1}{2l\pi} \int_{-l}^{l} \varphi(x)\,dx\,, \tag{2.1}$$

that is defined modulo 1 (as the phase φ is 2π periodic) and does not change while varying h_e for a given static solution.

International Electronic Journal of Pure and Applied Mathematics – IEJPAM, Volume 5, No. 4 (2012)

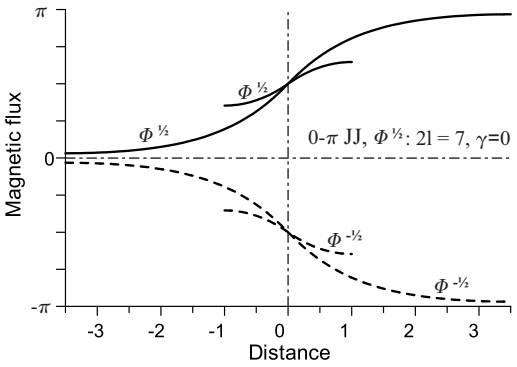

Figure 1: The Josephson phase $\varphi_0(x)$ corresponding to the static solution of the type $\Phi^{\pm 1/2}$ in 0-π JJ for $2l = 2$ and $2l = 7$ at $h_e = 0$ and $\gamma = 0$

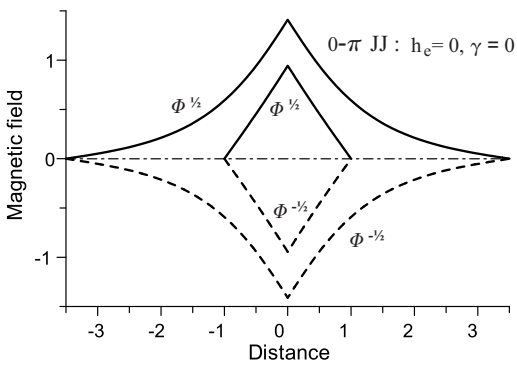

Figure 2: The magnetic field corresponding to the solutions shown in Figure 1

At the center $x = 0$ we have $\Phi^{\pm 1/2}(0) = \pm\pi/2$ (see Figure 1). Moreover, the conditions of geometrical symmetry are fulfilled:

$$\Phi^{-1/2}(x) = -\Phi^{1/2}(x),\ \frac{\partial\Phi^{-1/2}(x)}{\partial x} = -\frac{\partial\Phi^{1/2}(x)}{\partial x},\ \frac{\partial\Phi^{\pm 1/2}(x)}{\partial x} = \frac{\partial\Phi^{\pm 1/2}(-x)}{\partial x}.$$

In an "infinite" ($l \to \infty$) homogeneous 0-JJ the solutions $\Phi^{\pm 1/2}$ are reduced to pure (anti)semifluxon solution

$$\Phi_\infty^{\pm 1/2} = \begin{cases} 4\arctan\exp(x - x_0), & x < 0; \\ 4\arctan\exp(x + x_0), & x > 0, \end{cases} \tag{2.2}$$

where [5, 8] $x_0 = \ln\tan\frac{\pi}{8} = \ln(\sqrt{2} - 1)$.

In addition to the vortex solutions shown in Figures 1 and 2, at $h_e = 0$ and $\gamma = 0$ there exist also two Meissner's solutions $\varphi_0(x) = 0$ and $\varphi_\pi(x) = \pi$. They belong to the classes denoted as M_0 and M_π. The solutions of these classes can be obtained from $\varphi_0(x)$ and $\varphi_\pi(x)$ by continuation from $p = (l, 0, 0)$ to the given p provided we do not pass a bifurcation point. The solutions of the class $M_{0,\pi}$ have $\Delta\varphi = 0$ for $h_e = 0$ and $F[M_{0,\pi}] = 0, 4l$. The potential of SLP is $q(x) = \pm 1$. In particular $\lambda_0(0) \approx -0.3$ at $2l = 2$ and $\lambda_0(\pi) \approx -0.86$ for $2l = 7$ in accordance with [11]. Numerical experiment confirms, that Meissner's solutions remain unstable for all $h_e \neq 0$ and $\gamma \neq 0$, where they exist. Thus, in the case of 0-π JJ the traditional Meissner's branches are missed on the $\gamma_c(h_e)$ dependence as observed in experiment [16, 13].

International Electronic Journal of Pure and Applied Mathematics – IEJPAM, Volume 5, No. 4 (2012)

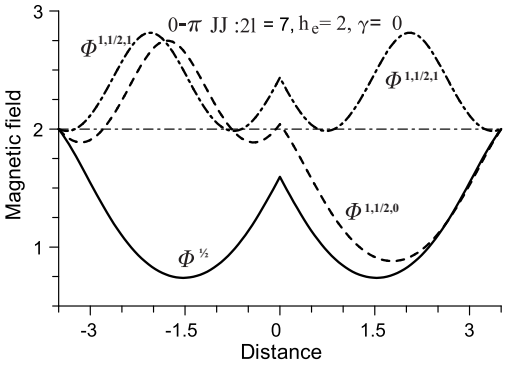

Figure 3: The magnetic field profiles corresponding to the bound states Φ^{M}, $\Phi^{1,1/2,0}$ and $\Phi^{1,1/2,1}$ in 0-π JJ of the length $2l = 7$ at $h_e = 2$

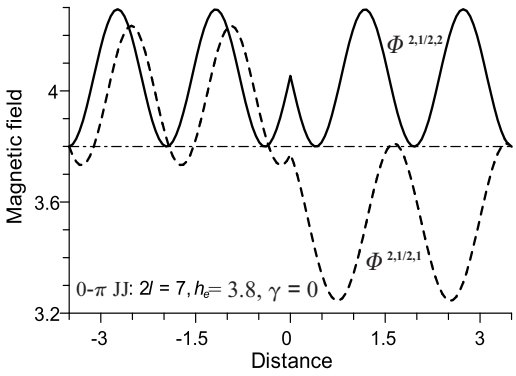

Figure 4: The magnetic field profiles corresponding to the bound states $\Phi^{2,1/2,2}$ and $\Phi^{2,1/2,1}$ at $h_e = 3.8$

By increasing the value of h_e some new, more complicated bound states may be observed. These states correspond to some fluxons present within 0 and π halves of LJJ with a semifluxon in the middle of the LJJ. We denote this type of static solutions as $\Phi^{L,M,R}$, where L (integer) is the number of fluxons in the left 0 part ($x < 0$), M (semi-integer) is number of fluxons pinned at $x = 0$ (usually it is (anti)semifluxon, i.e. $M = \pm 1/2$, the other semi-integer M are usually unstable) and R is the number of fluxons within the π part ($x > 0$). At $\gamma = 0$ each state $\Phi^{L,M,R}(x)$ has a mirror symmetric one $\Phi^{L,M,R}(x) = \Phi^{R,M,L}(-x)$ with the same energy and stability. If $L = R$, then it reflects into itself. This notation is a generalization of our previous notation, i.e., $\Phi^{0,M,0} \equiv \Phi^{M}$.

In Figure 3 for $h_e = 2$ and $\gamma = 0$ one can see examples of the states $\Phi^{1,1/2,0}$ with $N[\Phi^{1,1/2,0}] = 1.5$, $\Phi^{1,1/2,1}$ with $N[\Phi^{1,1/2,1}] \approx 2.5$. Similarly, in Figure 4 the states $\Phi^{2,1/2,2}$ have $N[\Phi^{2,1/2,2}] = 4.5$, and $\Phi^{2,1/2,1}$ $N[\Phi^{2,1/2,1}] = 3.5$ are shown.

On Figure 5 the dependence of $\lambda_0(h_e)$ is presented for selected classes of static solutions, i.e., $\Phi^{1/2}$, M_0, M_π. In accordance with (1.7) the zeroes of curves $\lambda_0(h_e, 0)$ are bifurcation points of the corresponding solutions. Each curve possesses two zeros which correspond to the lower $h_{\min}$ and upper $h_{\max}$ critical magnetic field for given type of solution and $\gamma = 0$. The distance $\Delta h = h_{\max} - h_{\min}$ represents the domain of stability of the particular type of solution $\Phi^{K,L,M}$ on the field h_e at $\gamma = 0$. For $\Phi^{\pm 1/2}$–distribution calculations yield $h_{\min} \approx -1.8$ and $h_{\max} \approx 2.2$, thus $\Delta h \approx 4$.

Similarly, in Figure 6 the behavior of the $\lambda_0(0, \gamma)$ for $2l = 7$ and $h_e = 0$ is demonstrated. Each branch corresponds to two symmetrical vortex distributions with the same λ_0 and same energy F, but with opposite total flux $\Delta\varphi$. Points

International Electronic Journal of Pure and Applied Mathematics – IEJPAM, Volume 5, No. 4 (2012)

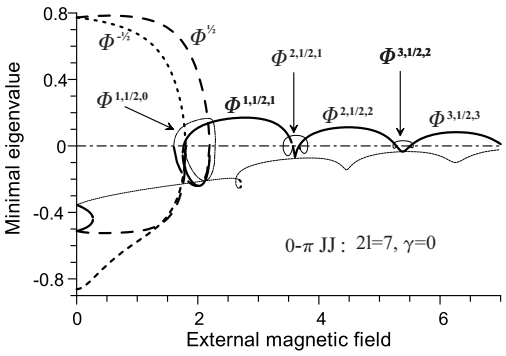

Figure 5: The dependence $\lambda_0(h_e)$ for several static solutions $\Phi^{L,M,R}$ in the 0-π JJ of length $2l = 7$ at $\gamma = 0$

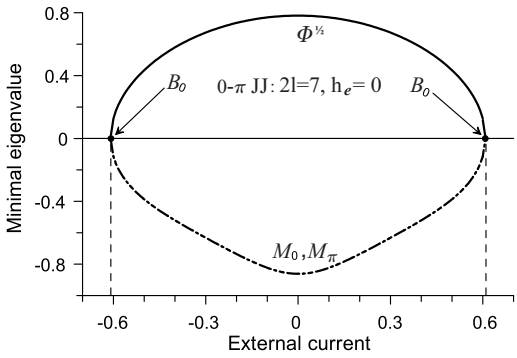

Figure 6: The dependence $\lambda_0(\gamma)$ for static solutions $\Phi^{1/2}$, $M_{0,\pi}$ in the 0-π JJ of length $2l = 7$ at $h_e = 0$

B_0 (situated exactly at $|\gamma| = 2/\pi$ for $l \to \infty$, see [23, 25, 10]) are the points of bifurcation with respect to parameter γ. At these points one can see a confluence of $\Phi^{\pm 1/2}$ solutions with $M_{0,\pi}$. For a given JJ, the distance between the points B_0 defines the domain of stability of semifluxon or antisemifluxon along γ.

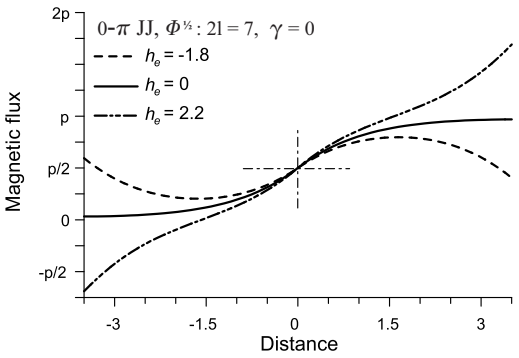

Figure 7: Magnetic flux distributions $\varphi(x)$ in the 0-π JJ of length $2l = 7$ at $\gamma = 0$

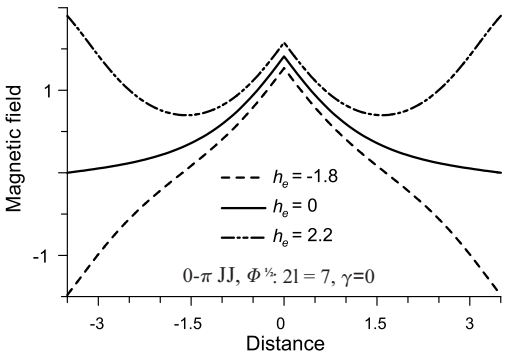

Figure 8: Magnetic field distributions $\varphi_x(x)$ in the 0-π JJ of length $2l = 7$ at $\gamma = 0$

Figures 7 and 8 illustrate the deformation of a semifluxon $\Phi^{1/2}$ by external magnetic field h_e in the 0-π JJ of length $2l = 7$ and $\gamma = 0$. According to the boundary conditions (1.1d) the main changes are localized near the edges of the JJ, while solution in the central part of the JJ remains almost unchanged.

International Electronic Journal of Pure and Applied Mathematics – IEJPAM, Volume 5, No. 4 (2012)

Similarly, in Figure 9 the deformation of the solution $\Phi^{1/2}$ by the bias current γ at $h_e = 0$ is presented. Positive current γ displaces the phase $\varphi(x)$ upwards (the maximum of the corresponding soliton $\varphi_x(x)$ moves to the left), and vice versa for the negative γ — the $\varphi(x)$ moves down, and the plot of $\varphi_x(x)$ shifts to the right.

The basic characteristics of several solutions of the type $\Phi^{L,M,R}$ in JJ with $2l = 7$ and $\gamma = 0$ are summarized in Table 1.

Type	h_e	λ_0	$N[\varphi]$	$\Delta\varphi/2\pi$	$\varphi(0)/\pi$	$F[\varphi]/8$
$\Phi^{0,-1/2,0}$	0	0.772	-0.5	-0.468	-0.5	-0.586
$\Phi^{0,1/2,0}$	0	0.772	0.5	0.468	0.5	-0.586
$\Phi^{1,1/2,0}$	1.61	0.0275	0.885	1.7	0.664	-1.349
$\Phi^{0,1/2,1}$	1.61	0.0267	2.115	1.7	2.336	-1.346
$\Phi^{1,1/2,1}$	2	0.108	2.5	2.582	2.5	-1.883
$\Phi^{1,1/2,2}$	3.41	0.015	2.897	3.773	2.771	-5.144
$\Phi^{2,1/2,1}$	3.41	0.012	4.103	3.773	4.229	-5.140
$\Phi^{1,1/2,2}$	4.6	0.111	4.5	5.049	4.5	-9.378

Table 1: Key characteristics of several solutions of the type $\Phi^{L,M,R}$

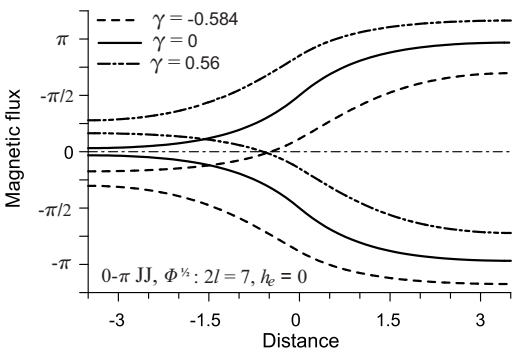

Figure 9: Magnetic flux distributions $\varphi(x)$ at $h_e = 0$

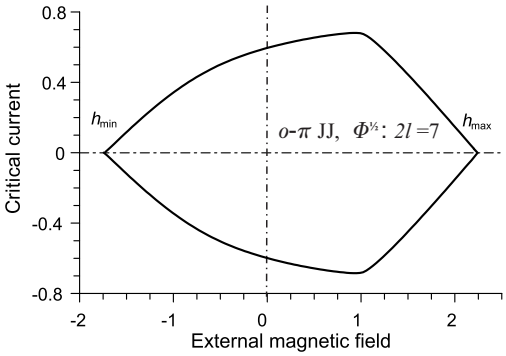

Figure 10: The bifurcation curve for the solutions $\Phi^{1/2}$ for $2l = 7$

2.2. Bifurcations of Static Solutions

Here we study bifurcations of static solutions varying external field h_e and external current γ. The locus on the plane (h_e, γ) satisfying equation (1.7), we shall call a bifurcation curve (BC). A unique BC corresponds to each solution type. An example

International Electronic Journal of Pure and Applied Mathematics – IEJPAM, Volume 5, No. 4 (2012)

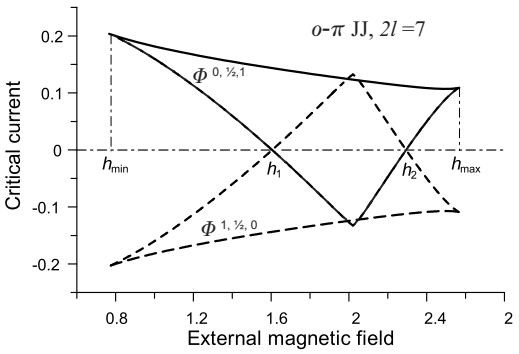

Figure 11: BCs of pairs $\Phi^{1,1/2,0}$ & $\Phi^{0,1/2,1}$ in 0-π JJ of length $2l = 7$

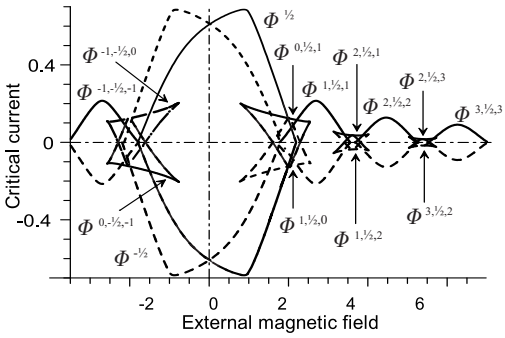

Figure 12: BCs for different types of static solutions in 0-π JJ of length $2l = 7$

of BC for $\Phi^{1/2}$ state is given in Figure 10. The distance $\Delta h_e \approx 4$ between zeroes $h_{\min} \approx -1.8$ and $h_{\max} \approx 2.2$ represents the region of stability of the $\Phi^{1/2}$ state. The profiles of magnetic field $\varphi_x(x)$ in a small neighborhood of the bifurcation points $h_{\min}$ and $h_{\max}$ are shown in Figure 8.

Similarly, in Figure 11 the BCs for $\Phi^{1,1/2,0}$ and $\Phi^{0,1/2,1}$ states are demonstrated. Note that the domain of stability has a triangular-like shape with sharp corners. For $\gamma = 0$ the stability interval (h_1, h_2) is smaller than for $\gamma > 0$, i.e., the bias current stabilizes these types of solutions.

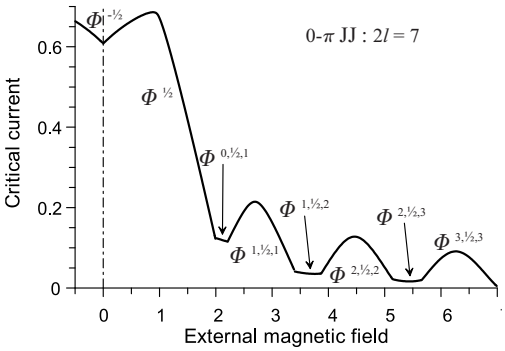

Figure 13: The envelope of the BCs for 0-π JJ of length $l = 7$. Due to the symmetry, only the right upper quarter on the γ–h_e plane is shown

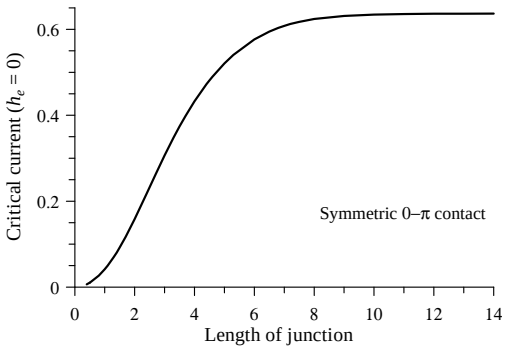

Figure 14: Critical current $\gamma_{c0}(0)$ as a function of length l

International Electronic Journal of Pure and Applied Mathematics – IEJPAM, Volume 5, No. 4 (2012)

The BCs for many types of static solutions discussed above are plotted in Figure 12 in a relatively large range of h_e.

In experiment one probably will not be able to see all the BCs shown in Figure 12 or one will not be able to trace any given BC completely. The reason is purely technical. One has to detect when the JJ passes a bifurcation point. If, after passing a bifurcation point, the JJ switches to the time-dependent solution with a non-zero average voltage $\langle\varphi_t\rangle$ (all such states we will call R-states), then one can detect it. This is usually done by measuring the maximum supercurrent as a function of applied magnetic field [19, 16, 13]. From Figure 12 it is obvious that if the absolute value of the bias current $|\gamma|$ at fixed h_e exceeds the the envelope of all bifurcation curves then there is no static solution and the JJ should switch to the R state. Thus, using voltage detection method one can at least see the envelope of BCs shown in Figure 13. Sometimes, especially for low damping, the JJ upon passing a bifurcation point for some state S_1 at γ_{c1} has a choice to switch either to the other static solution S_2 with $\gamma_{c2} > \gamma_{c1}$ or into the R state. If this will be an R state one will observe a BC of S_1, i.e., the value γ_{c1}. This ofetn happens in the visinity of the intersection of the two BCs corresponding to S_1 and S_2. Otherwise, the JJ switches from S_1 to S_2 and the decision is postponed up to the point γ_{c2} where the system will decide between S_3 and R states. We note, that some bifurcations curves contributing to the envelope, may not be visible in experiment because the static solutions associated with them are unstable at $\gamma = 0$ or at other "starting" value of γ, from where γ start the sweep to detect a transition to the R state. In fact, in experiment, the tracing may start not from $\gamma = 0$, but from other values, which may be even dynamically chosen. In this sense there, the experimental flexibility can be used to see hidden BCs rather than just the envelope.

However one can also use more advanced experimental technique, e.g., the one, which allows to measure magnetic flux in different parts of the 0-π JJ [39]. In this case one can easily trace the boundary bewteen zero voltage states different by the flux inside the JJ.

For a 0-π LJJ the value of the critical current at $h_e = 0$, i.e., $\gamma_{c0} = \gamma_c$ $(h_e = 0)$, depends on the LJJ length $2l$. The numerically calculated dependence $\gamma_{c0}(l)$ is plotted in Figure 14. For small l the critical current tends to zero as $\gamma_{c0} \approx \frac{1}{6}l^2$. At large l the current γ_{c0} asymptotically approaches the the constant value [6, 9, 10] $\gamma_{c0}^{\infty} = 2/\pi \approx 0.637$, while the total magnetic flux $\Delta\varphi(2l) \to \pi$, see [23, 25, 10].

3. Conclusions

For symmetric 0-π LJJs we numerically found the stability boundaries (bifurcation curves) on the "bias current – applied magnetic field" plane for different static solutions. This allows to predict the dependence of the critical current γ_c as a function of external magnetic field h_e and associate each branch of the experimental

International Electronic Journal of Pure and Applied Mathematics – IEJPAM, Volume 5, No. 4 (2012)

$\gamma_c(h_e)$ dependence with the stability boundary of a particular type of static solutions. Moreover looking at the overlap of different stability regions one can see what kind of states are possible in the different regions of parameter space and achieve these states experimentally even without measuring $\varphi(x)$.

We note that usual Meissner states $M_{0,\pi}$ are always unstable and do not contribute any bifurcation curve to Figure 12. We have also calculated the dependence of the critical current γ_{c0} at $h_e = 0$ on the length of the junction.

Acknowledgments

First author is grateful to Professor E. Goldobin for his important contribution in completing of this paper.

References

[1] L.N. Bulaevskii, V.V. Kuzii, A.A. Sobyanin, Superconducting system with weak link with a current in a ground state, *JETP Let*, **25**, No. 7 (1977), 290-294.

[2] V.V. Ryazanov, et al., Coupling of two superconductors through a ferromagnet: Evidence for a p junction, *Phys. Rev. Lett.*, **86** (2001), 2427.

[3] T. Kontos, et al., Josephson junction through a thin ferromagnetic layer: Negative coupling, *Phys. Rev. Lett.*, **89** (2002), 137007.

[4] J.J. A. Baselmans, et al., Reversing the direction of the supercurrent in a controllable Josephson junction, *Nature (London)*, **397** (1999), 43-45.

[5] L.N. Bulaevskii, V.V. Kuzii, A.A. Sobyanin, On possibility of the spontaneous magnetic flux in a Josephson junction containing magnetic impurities, *Solid State Commun.*, **25** (1978), 1053-1057.

[6] A.B. Kuklov, V.S. Boyko, J. Malinsky, Instability in the current-biased 0-π Josephson junction, *Phys Rev B*, **51**, No. 17 (1995), 11965-11968, Erratum, *Phys. Rev. B*, **55**, No. 17 (1997), 11878.

[7] R.G. Mints, I. Papiashvili, Josephson vortices with fractional flux quanta at $YBa_2Cu_3O_{7-x}$ grain boundaries *Phys. Rev. B*, **64** (2001), 134501.

[8] E. Goldobin, D. Koelle, R. Kleiner, Ground state and bias current induced rearrangement of semifluxons in 0-π long Josephson junctions, *Phys. Rev. B*, **67** (2003), 224515.

[9] E. Goldobin, D. Koelle, and R. Kleiner, Ground states of one and two fractional vortices in long Josephson 0-π junctions, *Phys. Rev. B*, **70** (2004),174519.

[10] E. Goldobin *et al.*, Fluxon-semifluxon interaction in an annular long Josephson 0-π-junction, *Phys. Rev. B*, **70** (2004), 094520.

[11] E. Goldobin, et al., Oscillatory eigenmodes and stability of one and two arbitrary fractional vortices in long Josephson 0-κ junctions, *Phys. Rev. B*, **71** (2005), 104518.

[12] E. Goldobin, et al., Josephson junction with magnetic-field tunable ground state, *Phys. Rev. Lett.*, **107**, No. 1 (2011), 22700.

[13] M. Kemmler, et al., Magnetic interference patterns in 0-π SIFS Josephson junctions: effects of asymmetry between 0 and π regions, *Phys. Rev. B*, **81** (2010), 054522.

[14] M. Knufinke, et al., Deterministic Josephson vortex ratchet with a load, *Phys. Rev. E*, **85** (2012), 011122.

[15] M. Weides, et al. High quality ferromagnetic 0 and π Josephson tunnel junctions, *Appl. Phys. Lett.*, **89** (2006), 122511.

[16] M. Weides, et al., 0-π Josephson tunnel junctions with ferromagnetic barrier, *Phys. Rev. Lett.*, **97** (2006), 247001.

[17] K. Buckenmaier, et al., Spectroscopy of the fractional vortex eigenfrequency in a long Josephson 0-π junction, *Phys. Rev. Lett.*, **98** (2007), 117006.

[18] H. Susanto, Darminto, S.A. van Gils, Static and dynamic properties of fluxon in a zig-zag 0-π Josephson junction, *Phys. Lett. A*, **361** (2007), 270-276.

[19] J. Pfeiffer, et al., Static and dynamic properties of 0, π, and 0-π ferromagnetic Josephson tunnel junctions, *Phys. Rev. B*, **77**, 21 (2008), 214506.

[20] M.B. Fogel, et al., Dinamics of sine-Gordon solitons in the presence of perturbations, *Phys. Rev. B*, **15**, No. 3 (1977), 1578-1592.

[21] Yu.S. Gal'perin, A.T. Filippov, Bound states of solitons in inhomogeneous Josephson junctions, *JETP*, **86**, No. 4 (1984), 1527-1543.

[22] A.T. Filippov, et al., Critical currents in Josephson junctions with micro inhomogeneities attracting solitons, *Phys. Lett. A*, **120**, No. 1 (1987), 47.

[23] T. Kato, M. Imada, Quantum effects of resistance-shunted Josephson junctions, *J. Phys. Soc. Japan*, **69** (2000), 203-212.

[24] T. Dobrowolski, An influence of the curvature on kink creation in the long Josephson junction, *Can. J. Phys.*, **88**, No. 9 (2010), 627-633.

International Electronic Journal of Pure and Applied Mathematics – IEJPAM, Volume 5, No. 4 (2012)

[25] B. Malomed, A. Ustinov, Creation of classical and quantum fluxons by a current dipole in a long Josephson junction, *Phys. Rev. B*, **69** (2004), 064502.

[26] N. Stefanakis and N. Flytzanis. Critical currents in Josephson junctions with macroscopic defects, *Supercond. Sci. Technol.*, **14** (2001), 16-29.

[27] I.V. Puzynin, et al., Methods of computational physics for investigation of models of complex physical systems, *Phys. Part. Nuclei*, **38**, No. 1 (2007), 70-116.

[28] T.L. Boyadjiev, M. Todorov, Minimal length of Josephson junctions with stable fluxon bound states, *Supercond. Sci. Technol.*, **15** (2002), 1-7.

[29] E.G. Semerdjieva, T.L. Boyadjiev, Yu.M. Shukrinov, Static vortices in long Josephson contacts of exponentially varying width, *J. Low Temp. Phys.*, **30**, No. 6 (2004), 610-618.

[30] E.G. Semerdjieva, M.D. Todorov, Fluxon centering in Josephson junctions with exponentially varying width, *East As. J. Appl. Math.*, **2**, No. 3 (2012), 204-213.

[31] A.N. Tikhonov, A.A. Samarskii, *Equations of Mathematical Physic*, Dover New York (1990).

[32] J. Keller, S. Antman, *Theory of Branching and Nonlinear Eigenvalue Problems*, Mir, Moscow (1974).

[33] A. Abrashkevich, I.V. Puzinin, CANM, a program for numerical solution of a system of nonlinear equations using the continuous analog of Newtons method, *Comp. Phys. Commun.*, 156 (2004), 154-170.

[34] T.L. Boyadjiev, Spline-collocation scheme of hight order of accuracy, JINR communications, Dubna, P2-2002-101 (2002).

[35] T.L. Boyadjiev, D.V. Pavlov, I.V. Puzynin, Newton's algorithm for calculation of the critical parameters in the one-dimensional inhomogeneous Josephson junction, *JINR communications, Dubna*, P11-88-409 (1988).

[36] T.L. Boyadjiev, D.V. Pavlov, I.V. Puzynin, Application of the Continiuos Analog of Newton Method for Computing the Bifurcation Curves in Josephson Junctions, in *Proc. Int. Conf. on Numumerical Methods and Applications, Sofia, August 22-27, 1988*, edited by Bl. Sendov, R. Lazarov, I. Dimov.

[37] I.V. Puzynin, et al., The generalized continuous analog of Newton method for numerical study of some nonlinear quantum-field models, *Phys. Part. Nuclei*, **30**, No. 1 (1999), 87-110.

International Electronic Journal of Pure and Applied Mathematics – IEJPAM, Volume 5, No. 4 (2012)

[38] I.V. Puzynin, et al., Methods of computational physics for investigation of models of complex physical systems, *Phys. Part. Nuclei*, **38**, No. 1 (2007), 70-116.

[39] A. Dewes, T. Gaber, D. Koelle, R. Kleiner, and E. Goldobin. Semifluxon molecule under control. *Phys. Rev. Lett.* **101** (2008), 247001.

International Electronic Journal of Pure and Applied Mathematics – IEJPAM, Volume 5, No. 4 (2012)